Received: 23 September 2022 | Revised: 2 February 2024 | Accepted: 22 March 2024

Micro & Nano Letters

DOI: 10.1049/mna2.12198

The Institution of Engineering and Technology WILEY

LETTER

Green synthesis and characterization of Ag nanoparticles using fresh and dry *Portulaca Oleracea* leaf extracts: Enhancing light reflectivity properties of ITO glass

Azeez A. Barzinjy[1,2] | **Banaz Sh. Haji**[1]

[1]Scientific Research Center, Soran University, Soran, Iraq

[2]Department of Physics Education, Faculty of Education, Tishk International University, Erbil, Iraq

Correspondence
Azeez A. Barzinjy, Scientific Research Center, Soran University, Kawa St., Soran, 44008, Iraq.
Email: azeez.azeez@soran.edu.iq

Abstract

Silver (Ag) nanoparticles (NPs) are perceiving remarkable progress during the past few periods due to its exclusive properties in many applications. Recently, green synthesis method of NPs is racing against traditional chemical and physical methods by avoiding the use of many toxic chemicals, and expensive devices. Accordingly, in this study, dry and fresh *Portulaca-oleracea* L. leaf extract has been employed for producing AgNPs as a reducing, capping and stabilizing agents. This process is simple, eco-friendly and green. UV–vis spectra showed the formation of AgNPs represented by the change of a colorless liquid to brownish solution. The crystallinity of the AgNPs, was confirmed by X-ray diffraction (XRD). The contribution of the available functional groups of the leaf extract in the reduction and capping process of NPs was demonstrated using Fourier transform infrared spectroscopy (FTIR). This study showed that fresh *Portulaca-oleracea* L. leaf extract provides better NPs in terms of stability, purity, degree of crystallinity and spherical shape. The biosynthesized AgNPs from both procedures were coated on the indium tin oxide (ITO) glass substrates to enhance the reflectivity property. It has been shown that the utilized AgNPs, from fresh *Portulaca-oleracea* L. extract, has smaller size and negligeable agglomeration, consequently lower light transmittance.

1 | INTRODUCTION

The field of nanotechnology is one of the supreme important field of investigation in recent material sciences [1]. Nanotechnology is a field that is emerging progressively, creating an impression in the entire sector of human life and generating a rising intelligence of delight in the life sciences, particularly biomedical procedures and biotechnology [2]. The term "nanoparticles" is utilized to define a particle with size in the range of 1–100 nm [3]. Based upon their type, size, shape, and structure, nanomaterials reveal a variety of inimitable electrical, optical, mechanical, magnetic, and antimicrobial properties, which have led to numerous fascinating industrial applications [4, 5]. Nowadays, metallic NPs have fascinated countless scientific attentiveness owing to their exclusive optoelectronic and physicochemical features with their requests in areas such as molecular diagnostics [6], drug carriage [7], imaging [8], solar cell [9], catalysis [10], and sensing [11].

In recent years, interest in silver nanoparticles (AgNPs) and their applications has increased dramatically as a result of their imperative properties [12]. In addition, AgNPs are one of the most talented harvests in nanotechnology manufacturing. AgNPs have some possible applications, such as indicative biomedical optical imaging [13], and medical request [14] such as wound bandages [15], clinical devices [16], food packaging [17], therapeutic applications [18], dental applications [19] and numerous key-purchaser belongings manufacturers that even now manufacture household substances that operate the antibacterial properties [20].

NPs synthesis is typically conducted by means of three main approaches: physical, chemical, and biological/green approaches [21]. Each of these methods possesses identifiable exclusive properties. Physical and chemical approaches are well thought out to be superior methods, especially in attaining steady nanostructures of identical dimension, however, they do not meet the purpose of obtaining longstanding

sustainability [22, 23]. Additionally, large-scale NP production can be achieved through the use of physical and chemical processes, but these approaches come at a significant cost because they demand a lot of energy. [24, 25]. Bearing in mind the restrictions of these approaches in nanomaterial synthesis, ecological approaches need to be settled utilizing procedures that are unpolluted, non-hazardous, and eco-friendly [26]. In other words, the production of NPs by physical and chemical methods requires the use of hazardous materials, advanced equipment, and has a negative impact on the environment. This has accompanied the development of "green nanotechnology" as a novel field. Biomanufacturing is a vital element of the green approach since it utilizes active organisms or biological parts as a replacement for costly physical or chemical approaches and delivers an ecologically harmless, and inexpensive technique for the synthesis of NPs. Biological or eco-friendly synthesis has been utilized as a green synthesis method for various range of NPs including metals, semiconductors, and quantum dots [27–29].

Phytochemicals or phytonutrients, are typically minor metabolites of plants with an extensive collection of chemical constructions, for example, alkaloids, saponins, indoles, phytosterols, phenolic acids, isothiocyanates, and phytoprostanes/furanes, proteins, and enzymes [30]. These metabolites are not indispensable for the growth and improvement of the plant, however, they are originated to be useful for human well-being and controlling illness [31, 32]. These phytochemicals, which can behave as a reducing and capping in addition to stabilizing agent for NP synthesis. Nevertheless, the mechanism of green synthesis methods is yet extremely arguable.

The biological synthesis of NPs involves of utilizing natural ingredients, including plants and microorganisms, which contain bacteria, algae, fungi, and yeast [33]. Microorganisms are essential platform that are able to accumulate and purify heavy metals due to the presence of various reductase enzymes that are able to reduce metal salts to metallic NPs [34]. The synthesis of NPs by bacteria has not yet been well investigated, although studies to date have shown that nanoparticles produced by bacteria have very good dispersion and stability and have significant lethal activity against various pathogens [35]. Algae is an extensively dispersed organism and its availability is abundant; an added advantage is their growth under laboratory conditions. These organisms can help with large-scale production at a low cost. Algae-mediated synthesis of NPs, along with the use of different capping agents, can help in modulating the stability and size of the NPs [36]. Fungi and yeast represent excellent frames for synthesizing NPs since they are very effective secretors of extracellular enzymes and a number of species grow fast [37]. Therefore, culturing and keeping them in the laboratory are very simple. Also, they are able to produce metal NPs via reducing enzymes intracellularly or extracellularly [38, 39]. Nevertheless, the available phytochemicals in plant extracts own an extremely extraordinary capacity for reducing metal ions in a limited period compared with bacteria, fungi, algae, and yeasts, which requires a longer growth time [40]. Accordingly, plant extracts have been prominent as a noticeable basis for synthesizing metallic NPs [41]. Moreover, the plant-refereed synthesis process for producing NPs is a primary procedure above the microorganism route owing to its effortlessness, quickness, and culture maintenance anticipation [42]. Also, plant extractions own an important status owing to comprising a great amount of phytochemicals, for instance, flavonoids, glycosides, polyphenol, terpenoids, and enzymes, which behave as reducing, capping, and stabilizing agents [43]. Furthermore, biological synthesis offers an ecofriendly construction of NPs of diverse dimensions and natures [44–46].

The biosynthesizing NPs initially started using dry plants as reducing and capping agents [47, 48]. The advantage of utilizing dried plants is that the plant can be stowed for a long time at ambient temperature till required. However, the fresh plant ought to be stowed at 20° below 0°C to avoid degradation [49]. Also, the dried plant is more desirable owing to variances in water content inside the plant tissues [50]. Similarly, the impacts of periodic variants, which cause deviations in plant ingredients are excluded by means of dried ingredients. Oikeh et al. [51] stated that fresh plant extract contains more and active phytochemicals than the dried plant extracts. Indeed, there are several parameters affecting the size, morphology, and number of created NPs. Among these parameters; plant extract and metal slat concentration, in addition to modifying the pH, reaction temperature, and time [52].

With the intention of resolving the energy shortage and environmental pollution issues, the actual use of solar energy has become extremely significant. Since the energy density of sunlight is low and uneven, increasing the absorption and efficiency of sunlight is important for the efficient conversion of solar energy. Numerous methods and materials have been industrialized to operate more sunlight. Amongst them, surface plasmon resonances of nanometals have concerned abundant consideration since their procedure is easy, reproducible, and effective route and can be used in large scale construction [53]. In this study, an effective technique was used to coat Ag NPs on indium tin oxide (ITO) glass using the spin coating method.

The novelty of this study is that Ag NPs can be synthesized from an easy reaction without using any external stabilizing and reducing agent, which is not possible through traditional procedures. This study also is rare and distinctive, and it demonstrates that the process of NPs formation is not clear and there are many parameters affecting the structural, chemical and optical properties of the NPs. Therefore, this study which is a continuation of our recent works [47, 54–63] originally conducted to compare the impact of dried and fresh leaf extracts of *Portulaca oleracea* L. on structure, size, morphology, purity, degree of crystallinity and optical properties of Ag NPs. Finally, this study was aimed to utilize Ag NPs, from fresh and dry *P. oleracea* L. leaf extracts, to enhance light reflective properties of ITO glass.

2 | MATERIALS AND METHODS

2.1 | Fresh and dry *P. oleracea* L. leaf Extract

In this study, *P. oleracea* L. has been selected since this plant has been qualified as a unique food of future. It is remarkable that no sign of notable toxicity of this plant has been reported yet

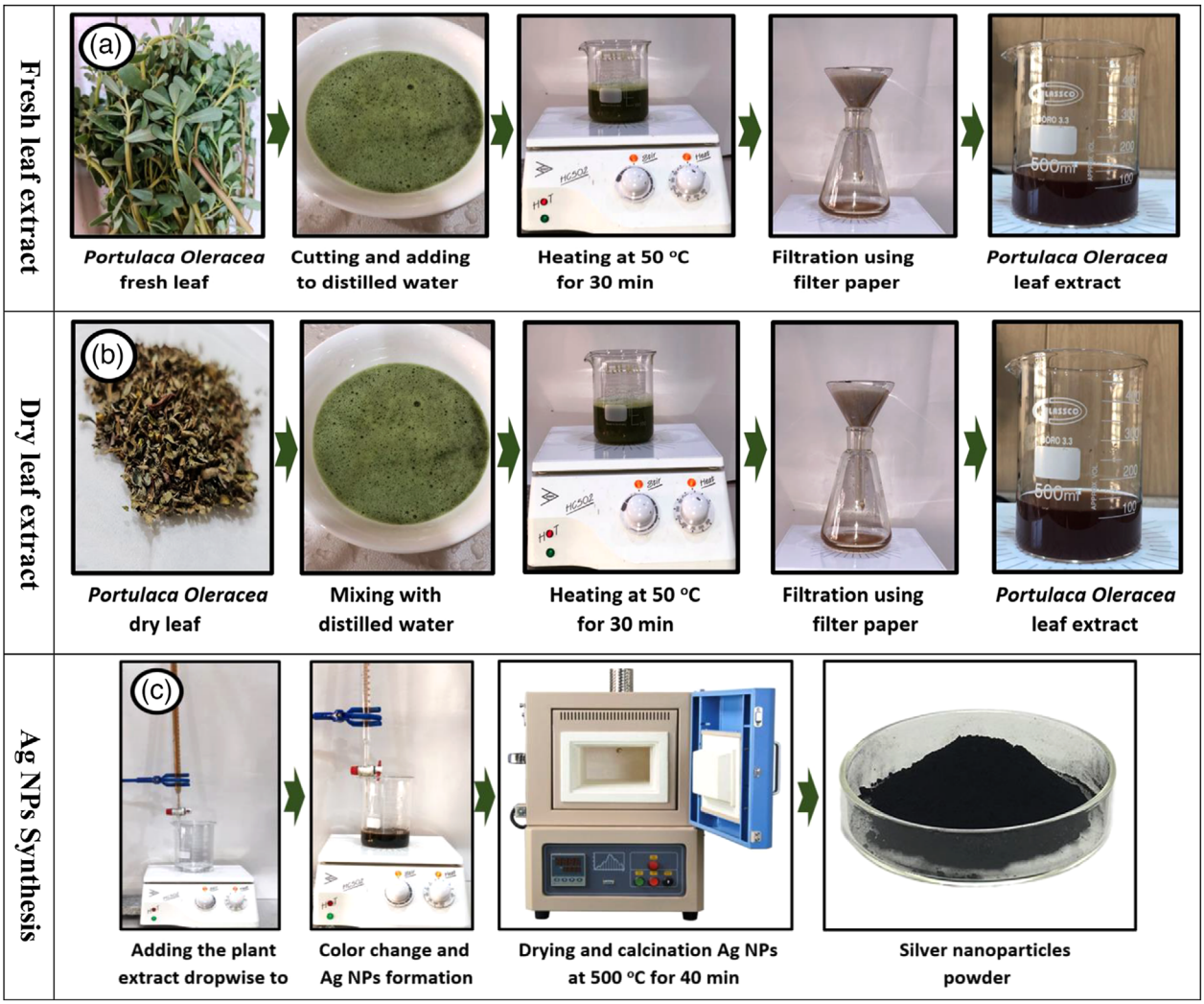

FIGURE 1 Preparation process of (a) fresh, (b) dry *Portulaca oleracea* L. leaf extract and (c) Ag NPs from fresh and dry *Portulaca oleracea* L. extracts.

[64]. *P. oleracea* L. is a rich source of α-linolenic acid, omega-3 fatty acids, ascorbic acid, β-carotene, α-tocopherols, phenolic alkaloids, glutathione and many other components. Accordingly, this plant is contains reducing, capping and stabilizing agent. Five grams of fresh *P. oleracea* L. leaves were carefully washed in distilled water, cut into sufficient fragments then saturated in a flask contained 100 mL distilled water. The mixture was heated at 50°C for 30 min (Figure 1a). The extract was permitted to turn cold at room temperature and then clarified using filter paper to eliminate undesirable organic ingredients.

Five grams of dry *P. oleracea* L. were saturated in a flask enclosed 100 mL of distilled water. The mixture was heated at 50°C for 30 min (Figure 1b). The extract was permitted to calm down to room temperature and then clarified with filter paper to eliminate undesirable organic ingredients.

2.2 | Synthesis of silver nanoparticles

The quantity of 0.25 g of silver nitrite was liquefied in 50 mL double distilled water and reserved stirring for 20 min at 60°C. This ratio is a standard silver solution for Ag NPs preparation [65]. Then, 50 mL of both fresh and dry *P. oleracea* L. extract solutions were drop wise added to the liquefied silver nitrite individually. The last mixtures were put on the hotplate, heated, and stirred at 70°C for 40 min till the colour of the mixtures altered to a brownish colour (Figure 1c). The acquired ingredients were disconnected from the combination by centrifugation at 7000 rpm for 25 min and later heated at 500°C in muffle furnace for 40 min by means of an oven to eliminate all of the contamination and organic ingredients nearby the Ag NPs.

The biosynthesizing process of Ag NPs could be discussed as follows: first, the reduction of silver metal salt ions into silver metal atoms; second, the growth and nucleation of Ag NPs with a specific size and shape; third, the steadiness step, wherein the phytochemicals cover and prevent NPs from aggregation by secondary metabolites of plant extraction, and finally the calcination of the Ag NPs to remove all unwanted impurities around the Ag NPs. Figure 1c represents the graphical representation of the Ag NPs formation using fresh and dry *P. oleracea* L. extract. This approach can be extended to prepare other noble metal NPs, such as Au and Pt.

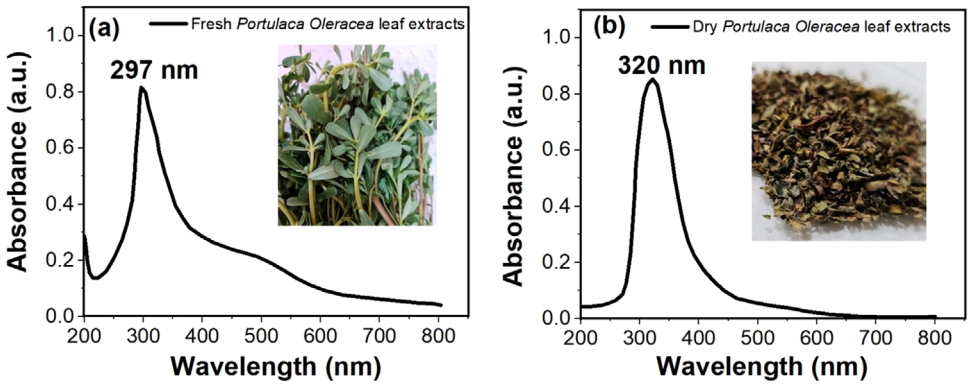

FIGURE 2 UV Spectrum for (a) fresh and (b) dry *Portulaca oleracea* L. leaf extracts.

2.3 | Samples characterization

To explore the crystal structure of arranged Ag NPs, X-ray diffraction (PAnalytical X' Pert PRO, Cu $K\alpha = 1.5406$ Å) was used. The scanning level was 1°/min in the 2θ range from 20° to 80°. In addition, the visual characteristics of the Ag NPs samples were also investigated through the double beam UV–vis (Super Aquarius Spectrophotometer-1000) with a deuterium and tungsten iodine lamp in the range of 200 to 900 nm at room temperature. The morphology of the samples was studied through field emission scanning electron microscopy (SEM Quanta 450). The elemental configuration of the Ag NPs nanostructures was determined by energy-dispersive X-ray spectroscopy (EDX) implemented in the SEM instrument. The composition and organic molecules around the growth of Ag NPs nanostructures were analysed by means of Fourier transform infrared (Perkin Elmer FTIR) spectrophotometer in the acquisition assortment of 400–4000 cm^{-1}.

3 | RESULTS AND DISCUSSION

3.1 | Characterization of plant extracts

3.1.1 | UV–vis spectra of dry and fresh *P. oleracea L.* leaf extracts

UV–vis method is at the same time qualitative and quantitative analysis. It is a rapid, initial, and important step for determining the ability of a plant to prepare the NPs. Numerous phytochemicals are available in plant extracts that result in metal ion reduction and the formation of NPs. These phytochemicals are, also, contributing to the formation, capping, and stabilization of NPs [66]. Reducing agents reduce the metal ions to metal zero, while capping agents stick to the NPs surface through either covalent bonds or interaction. Capping agents protect NPs from aggregation. Normally, the UV–vis absorption range between 200–400 nm is the optimum range for phytochemicals screening in plant extracts. For instance, flavonoid possesses two absorption maxima in the ranges of 230–285 nm and 300–350 nm [67]. Comparable consequences were found in a previous investigation [68] stating that the UV-Vis spectrum of leaf extract in the absorption range of 270–340 nm.

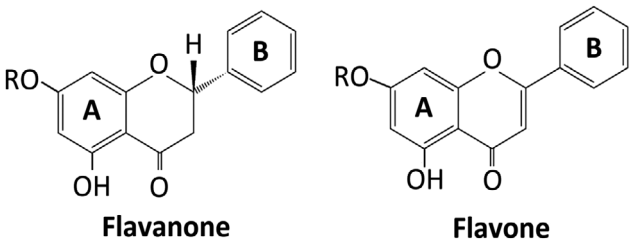

FIGURE 3 Chemical construction of flavanone and flavone.

Figure 2 shows the UV–vis spectra of fresh and dry *P. oleracea* L. leaf extracts. This investigation showed that the phytochemicals in fresh leaf extract of *P. oleracea* L. possess a maximum UV peak at 297 nm (Figure 2a). Zhu et al. [69] stated that flavonoids are one of the leading energetic components of *P. oleracea* L. Therefore, this peak is more likely to belong to flavanone.

Flavanone is a type of a type of flavonoids, is an aromatic and colourless ketone consequential from flavone that frequently arises in plants as glycosides [70]. It can be noticed from Figure 2b that the highest UV peak, for the dry *P. oleracea* L. leaf extract is shifted from 297 to 320 nm. This is, perhaps, due to the availability of flavone instead of flavanone (Figure 3).

The alteration of flavanone to flavone affects the formation of nanoparticles in a very many-sided manner. This is verified by the disturbance of the pairing of the arrangement, which leads to the perturbation of the acidity and thus the acceptance of the hydrogen bond and the donating capacities of the OH groups, which are alcoholic in flavanones and phenolic in flavones, possibly both of which are related to flavonoids [71]. As stated by Donkor et al. [72] the flavonoid spectra predominantly involve two absorption UV maxima, the first one between 200 and 299 nm and the second one between 300 and 350 nm. Rani et al. [68] stated that the UV–vis range of leaf extract in general is in the absorption assortment of 270–340 nm.

3.1.2 | FTIR spectra of dry and fresh *P. Oleracea* leaf extracts

To study the functional groups of *P. oleracea* L. leaf extracts, a FTIR investigation was conducted and the spectra is shown in Figure 4. The FTIR spectra of dry and fresh *P. oleracea* L. leaf

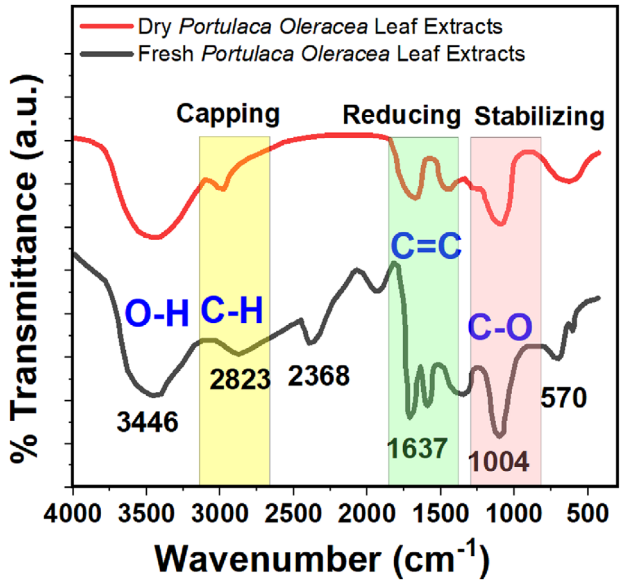

FIGURE 4 FTIR spectra of dry and fresh *Portulaca oleracea* L. leaf extracts.

extracts exhibit absorption peaks positioned between 4000 and 500 cm^{-1}. The most intense and broad peak in both spectra is positioned at 3446 cm^{-1}, which matches the O—H stretching. This peak in the fresh leaf extract of the *P. oleracea* L. plant is comparable to the corresponding peak in the dry leaf extract of *P. oleracea* L. plant. This is more likely due to the similar O—H groups in both flavanone and flavone compounds. The peak positioned at 2823 cm^{-1} is belong to the C—H stretching. This peak indicates the available capping agents in the plant extract. Capping agents are accountable to impede uncontrollable NPs from growing, controlling agglomeration, and solubility in various solvents. It can be perceived, from Figure 4, that this peak is broader in the fresh extract of *P. oleracea* L. than the dry extract of *P. oleracea* L. plant. It can be stated that the capping agents not only govern the particle dimension, agglomeration, and morphology but also the steadiness of NPs over time [73]. The band at 1637 cm^{-1} is allocated to C═C vibration group. This peak is identifying the reducing agents available in the fresh and dry extracts of *P. oleracea* L. The key role of the reducing agent is offering the electrons for the available ions to form zero valent atoms. Then these atoms will combine together to form a NP. The located group at 1004 cm^{-1} belongs to the C—O stretching. This peak represents the stabilizing agent in the plant extract. The FTIR range of the fresh extract of *P. oleracea* L. has more details than the dry extract of *P. oleracea* L. This is most probably due to the fact that, throughout the dehydration process, the plant extract will lose some volatile phytochemicals and the chemical composition of the plant will change [74]. This, in turn, affects directly the structure, morphology, optical properties, and the size of biosynthesized NPs.

3.2 | Characterization of Ag NPs

Numerous functional factors, including microbial source, reaction temperature, pH, pressure, incubation time, and metal salt concentration, affect the synthesis of the NPs. Optimization of these parameters is required for the synthesis of NPs with accurate size, morphology, and chemical compositions. After the synthesis of NPs, purification before their use in any application is also essential. Typically, repeated washing and high-speed centrifugation are performed to separate and enrich the produced NPs and to eliminate unreacted bioactive molecules [75].

3.2.1 | UV–vis spectrum of the green synthesized Ag NPs

UV–vis spectroscopy is one of the significant description methods to investigate the optical characteristics of NPs. This method agrees to confirm the NPs formation through assessing the surface plasmon resonance (SPR) [76]. UV–vis spectroscopy can offer evidence regarding the size, band gap, steadiness, and agglomeration status of the NPs [77]. The wavelength range between 200 and 700 nm is commonly utilized to describe the metal and metal oxide NPs. Ag NPs, normally, display an explicit absorption peak among 400 and 450 nm [78]. Figure 5 displays the UV–vis spectrum of biosynthesized Ag NPs using fresh and dry extract of *P. oleracea* L. It can be realized, from Figure 5, that the Ag NPs have been formed using both

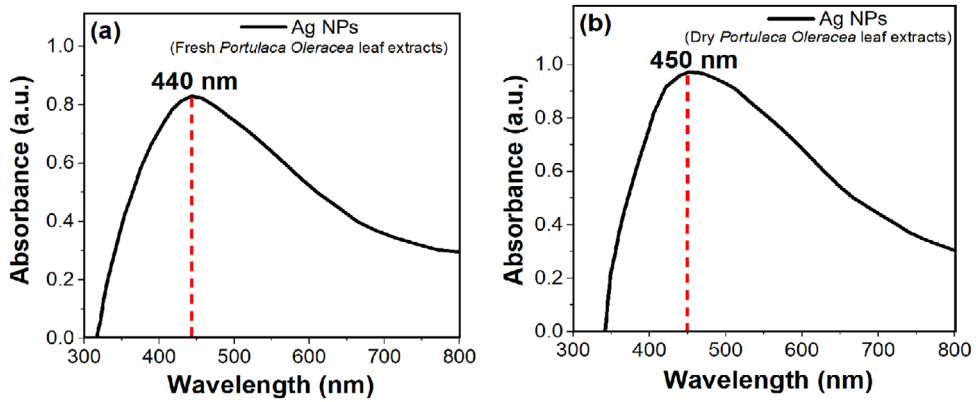

FIGURE 5 UV–vis spectra of Ag NPs synthesized from (a) fresh and (b) dry *Portulaca oleracea* L. leaf extracts.

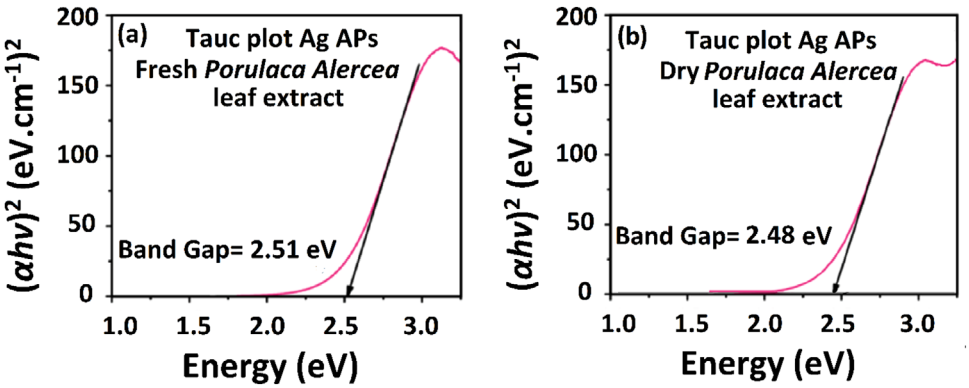

FIGURE 6 Energy band gap of Ag NPs synthesized from (a) fresh and (b) dry *Portulaca oleracea* L. leaf extracts.

extracts. However, the maximum absorption peak appeared at 440 nm using fresh *P. oleracea* L. extract and 450 nm using dry *P. oleracea* L. extract. It can be noticed that these standards are inferior than those of bulk Ag particles, which normally appear at 520 nm [62]. Another remarkable point one can deduce from Figure 5 is that in both cases, the UV–vis peaks are broad indicating to the polydisperse Ag NPs which can be further clarified in the SEM section. It is generally accepted that, biological syntheses of NPs utilizing plant extracts yield polydisperse NPs through various features that are not easy to control from the organic perspective [62, 79, 80]. According to our best knowledge, the concentration and type of the utilized plant extract, the amount and nature of the utilized salt, pH, reaction time, and reaction temperature all affect the degree of generating macromolecules during the nucleation period, which affects directly the degree of mono/polydispersity of NPs and later decreases the synthesizing rate [81]. Since, in this investigation, all the steps to obtain Ag NPs were fixed except for the observation of the effect of using fresh and dry *P. oleracea* L. leaf extract, therefore the polydispersity state was comparable. It can be stated that the polydispersity of NPs is significant from a practical point of view where NPs size variation is required [82, 83]. In some circumstances, the impact of polydispersity might be useful, particularly, for discriminating the adsorption of tiny species [84].

3.2.2 | Band gap energy of the green synthesized Ag NPs

Band gap possesses a vital role in the electrical and optical characteristics of nanomaterials. Nanomaterials possess wide requests owing to their wide-ranging band gaps. It can be noticed that as the particle dimension reduces, the number of atoms or molecules in the NPs drops, hereafter, the orbitals overlapping will decrease. This, in turn, makes the valence and conduction bands narrower [85]. Accordingly, for NPs, once the width of the valence and conduction bands drops, the band gap amongst the valence and conduction bands will increase [86]. In other words, once the band gap is increased, the electron movement is restricted and the quantum confinement becomes obvious [87]. In metallic NPs, the conduction electrons are not completely free as in the bulk construction, alternatively, some of the electrons are held by the distinct atoms and more or less are free and can move amongst atoms to make metallic-bonds that strengthen the metallic NPs [88]. Once these metallic NPs are subjected to the ultraviolet (UV) light, the conduction electrons practice intra-band quantum excitations outside the Fermi-energy level, from which the conduction band of metallic NPs is distinct [89]. The energy band gap of the green synthesized Ag NPs from fresh and dry *P. Oleracea* leaf extract was found from the Tauc plot by inferring the rectilinear relation of the UV–vis curvature (Figure 6). The data are taken from Figure 5, the *x*-axis represents the wavelength, and is converted to the energy using Planck's equation, that is, $E = hc/\lambda$ and plotted in Figure 6. Where h is Planck's constant $= 6.62 \times 10^{-34}$ J/s, c is the speed of light $= 3 \times 10^{8}$ m/s and λ is the wavelength. While the absorbance, the *y*-axis in Figure 5, is converted to $(\alpha h\nu)^2$ in Figure 6, where α is the absorbance and ν is the frequency $\nu = c/\lambda$. It can be perceived, from Figure 6, that the biosynthesized Ag NPs from fresh *P. oleracea* L. leaf extract possesses higher band gap, 2.51 eV, than the biosynthesized Ag NPs from dry *P. oleracea* L. leaf extract, 2.48 eV. This is more likely owing to the NPs size effects, as the Ag NPs size using fresh extract is smaller than the Ag NPs size using dry extract of *P. oleracea* L. Normally, smaller NPs size lead to fewer numbers of atoms and hence the attraction force between the conduction electrons and metallic ions becomes smaller. Thus, the energy band gap increases with decreasing the particle size [90]. Equally, bigger NPs size contain bigger number of atoms, therefore the attraction force between the conduction electrons and metallic ions becomes bigger. Thus, the energy band gap decreases with increasing particle size [91]. The band gap increment in Ag NPs undoubtedly have potential applications in progressive optoelectronic equipment, thermal requests, batteries, and sensors [92]. The outcomes of this investigation are comparable to the previously reported investigations [93, 94].

3.2.3 | FTIR spectra of biosynthesized Ag NPs

The FTIR spectroscopy was conducted to classify the probable biomolecules that are in charge for reducing, capping and stabilizing agents of the biosynthesized Ag NPs using fresh

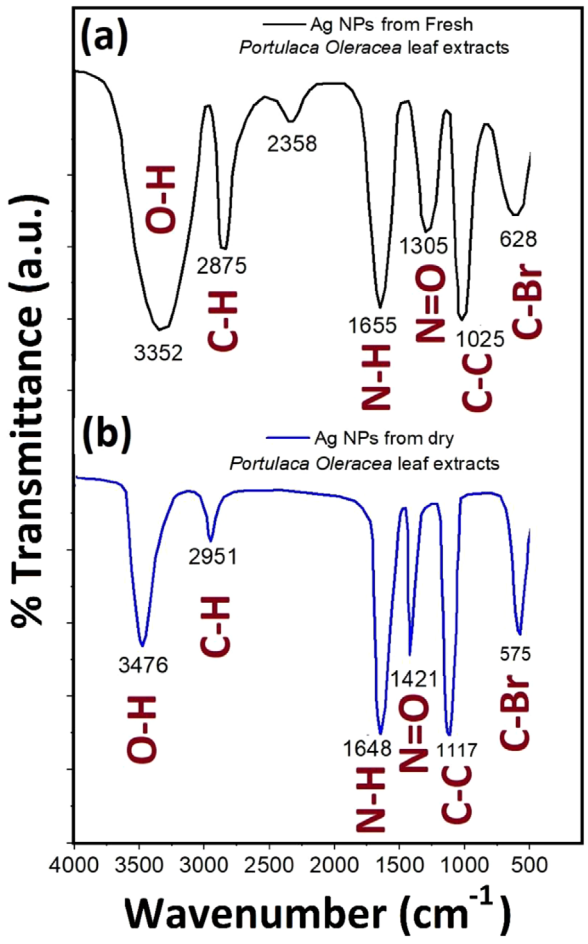

FIGURE 7 FTIR spectra of Ag NPs biosynthesized from (a) fresh and (b) dry *Portulaca oleracea* L. leaf extracts.

and dry *P. oleracea* L. leaf extract. The strong broad band, in Figure 7, at 3352 cm^{-1}, using fresh *P. oleracea* L. leaf extract, and 3476 cm^{-1}, using dry *P. oleracea* L. leaf extract, are owing to the O—H stretching mode. It can be noticed, from Figure 7, that this peak is broader using fresh *P. oleracea* L. leaf extract than the dry *P. oleracea* L. leaf extract due to having more hydroxyl group groups in the fresh plant extracts. The wide absorption band at 3326 cm^{-1} was also found by Senthil et al. [95] to the O—H group using pure fenugreek leaf extract. In addition, the peaks at 2875 cm^{-1}, using fresh *P. oleracea* L. leaf extract, and 2951 cm^{-1}, using dry *P. oleracea* L. leaf extract, is more likely as a result of the aldehydic C—H stretching mode. Comparable results were found by He et al. [96] using *hrysanthemum morifolium* Ramat. extract at room temperature. The lonely band at 2358 cm^{-1}, only appeared using fresh *P. oleracea* L. leaf extract, is possibly resulting from the distortion vibration C—H delimited in the acetyl collection [97]. The peaks at 1655 cm^{-1}, using fresh *P. oleracea* L. leaf extract, and 1648 cm^{-1}, using dry *P. oleracea* L. leaf extract, match up with the N—H bend primary amines. A similar interpretation has been stated by Mallikarjuna et al. [98] once they synthesized Ag NPs from *Ocimum* leaf extract. The peaks that appeared at 1305 cm^{-1}, using fresh *P. oleracea* L. leaf extract, and 1421 cm^{-1}, using dry *P. oleracea* L. leaf extract are associated with N═O regularity stretching, which is representative of nitro multifaceted [99]. Moreover, the peaks at 1025 cm^{-1}, utilizing fresh *P. oleracea* L. leaf extract, and 1117 cm^{-1}, using dry *P. oleracea* L. leaf extract, are related to C—N and C—C stretching, signifying the existence of protein amines [22]. Generally, the protein attachment to the Ag NPs sustains the steadiness of Ag NPs significantly over performing as capping and stabilizing agents and accordingly defending them from agglomeration [22]. To end with, the peaks at 628 cm^{-1}, using fresh *P. oleracea* L. leaf extract, and 575 cm^{-1}, using dry *P. oleracea* L. leaf extract, is attributed to C—Br stretching, which is characteristic of alkyl halides [100]. Additional studies stated that peaks at insignificant field in the range 400–700 cm^{-1} imitated the metallic behaviour of any inspected sample, Ag NPs in this study [101]. As indicated previously, these purposeful groups, as an over-all rule, possess a starring role in the stabilizing and capping of Ag NPs, as described in numerous investigations [102–105].

3.2.4 | XRD analysis of biosynthesized Ag NPs

Investigation over X-ray diffraction was conducted to approve the crystalline behaviour of the Ag NPs biosynthesized from both fresh and dry *P. oleracea* L. leaf extract. Figure 8 displays the X-ray diffraction configuration for the fresh and dry *P. oleracea* L. Ag NPs. It can be perceived, from Figure 8, that the XRD peak locations for fresh and dry *P. oleracea* L. The diffraction peaks at 38.01°, 44.34°, 65.52°, and 77.30° are linked to the (111), (200), (220), and (311) planes, in that order. These diffraction peaks, of a cubic crystal system ($a = 4.0686$ Å) have been coordinated with the typical JCPDS card No. 65–2901to monitor the purity and crystalline degree of Ag NPs from both sources. It can be seen, from Figure 8a, that unlike utilizing dry *P. oleracea* L. leaf extract no extraneous Bragg reflections were detected in the configuration, with utilizing fresh *P. oleracea* L. leaf extract, owing to crystallographic contaminations in the sample, which shows the existence of 100% unadulterated metallic Ag NPs in the sample [106]. This is a respectable pointer that, unlike the dry *P. oleracea* L. extract, fresh *P. oleracea* L. extract, yields unadulterated, high-quality, and steady NPs. Another point from Figure 8 that attracts our consideration is that the (111) plane is predominant in both cases since it displays high intensity. This is a clear indicator that the alignment of the crystal growth is mainly lengthwise the (111) plane. Narrowing of the diffraction peak reveals the formation of pure crystalline Ag NPs [107]. The correlation between XRD analysis (Figure 8) and FTIR analysis (Figure 7) indicates that the smaller abundance of the OH group in the dry *P. oleracea* L. extract leads to the formation of exotic peaks in the XRD spectrum. These exotic peaks, indicated by the red arrows, are more likely belong to $AgNO_3$ rather than the formation of Ag NPs.

The Debye–Scherrer equation consistent with the XRD pattern (Figure 8) was utilized to compute the crystalline dimension of the Ag NPs:

$$D = \frac{0.94\,\lambda}{\beta \cos\theta}$$

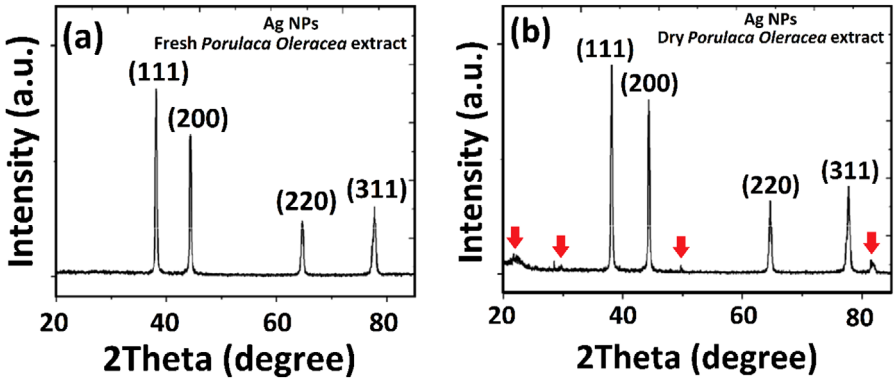

FIGURE 8 XRD configuration of Ag NPs synthesized from (a) fresh and (b) dry *Portulaca oleracea* L. leaf extracts.

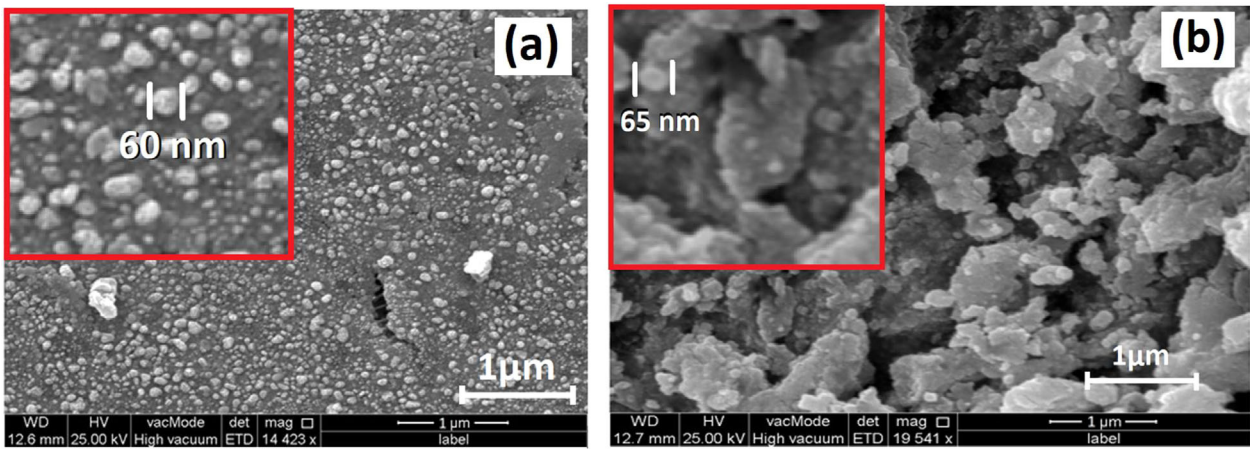

FIGURE 9 SEM descriptions of Ag NPs synthesized from (a) fresh and (b) dry *Portulaca oleracea* L. leaf extracts.

where D is the regular crystallite dimension of the NPs, the wavelength of the incident X-ray, that is λ is 0.154 nm, θ is the Bragg's angle, and β is the full width at half maximum (FWHM). It can be stated that, the narrow FWHM, is a clear sign of the availability of a high crystalline construction of NPs. The regular crystalline dimension, Debye Scherrer equation, of the Ag NPs using fresh and dry *P. oleracea* L. leaf extract was around 45 and 50 nm, respectively. Analogous consequences have been obtained by other investigators [108, 109]. In general, the crystalline dimension is comparatively slighter than the grain dimension, which might be attained through the scanning electron microscope (SEM) [62].

3.2.5 | SEM and EDX analysis of green synthesized Ag NPs

The morphological investigation of the green synthesized Ag NPs was inspected through scanning electron microscopy (SEM) technique. The SEM descriptions of the Ag NPs, using fresh and dry *P. oleracea* L. leaf extract is presented in Figure 9. It can be realized that the majority of Ag NPs, of both systems, possess nanoscale size, distinct structures and obvious spherical morphology. In addition, the grain dimension of the green synthesized Ag NPs by means of fresh *P. oleracea* L. leaf extract is relatively smaller than the Ag NPs via dry *P. oleracea* L. leaf extract. This is expected since the dehydration process is directly affecting the performance of the plant extract and, as stated before, the plant might lose some volatile phytochemicals that affect the NPs formation process [110]. Moreover, the agglomeration status of the Ag NPs using fresh *P. oleracea* L. leaf extract, is considerably lower than the dry *P. oleracea* L. leaf extract case. This is, most probably, due to existence of more protein, acting as capping agents, in the fresh extract rather than dry extract which directly reduce the agglomeration state during the NPs formation [111]. On the other hand, as indicated in the UV–vis and FTIR investigation, using dry plant extract causes a non-uniform nucleation procedure and therefore creating the agglomerated bunches. Alternatively, agglomeration is typically due to the extraordinary surface energy per unit volume proportion, which exists in the majority of the green synthesized NPs [112]. Also, the reactivity and agglomeration of NPs are mostly dependent on their particle size. It is well known that the process of agglomeration will happen at slower rates in smaller

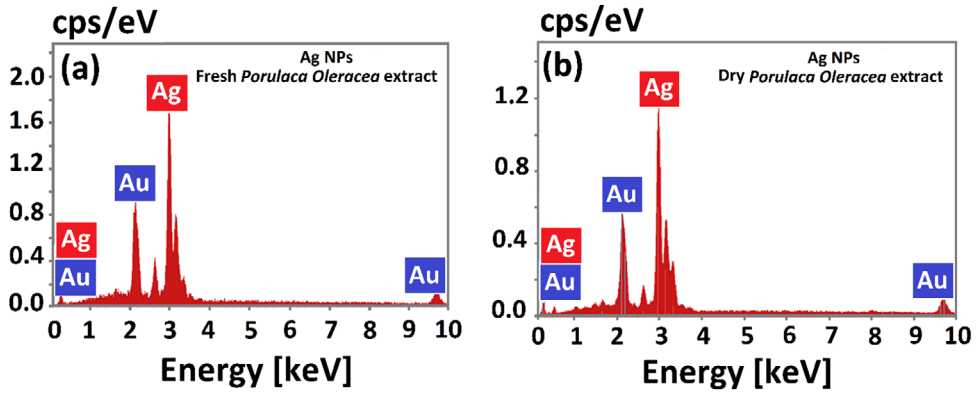

FIGURE 10 EDX analysis of Ag NPs synthesized from (a) fresh and (b) dry *Portulaca oleracea* L. leaf extracts.

particles [113]. The correlation between structural, XRD, analysis (Figure 8) and morphological, SEM, analysis (Figure 9) indicates that the Ag NPs synthesized by fresh *P. oleracea* L. leaf extract possess a higher degree of crystallinity than the Ag NPs synthesized by dry *P. oleracea* L. leaf extract. Thus, the foreigner peaks, which belong to $AgNO_3$ rather than the formation of Ag NPs, are responsible for irregular nucleation and growth processes, and hence increasing the degree of agglomeration.

The elemental exploration of the green synthesized Ag NPs was studied through energy dispersive X-ray (EDX) analysis. The EDX ranges (Figure 10) display a robust indication in the Ag region, that is, 3 keV, and approve the creation of Ag NPs and its elemental behaviour. This indicator was formed owing to the excitation of surface plasmon resonance of the biosynthesized Ag NPs. More or less of the feeble indicators from gold were noticed. These indications were shaped as a result of coating the Ag NPs with a 100 Å layer of Au to improve the SEM images quality. Figure 10, also, displays the pureness of the green synthesized Ag NPs, consuming both fresh and dry *P. oleracea* L. leaf extract, which comprises merely metallic Ag without contamination from the other substances. The higher intensity from the fresh *P. oleracea* L. leaf extract is clear evidence that fresh *P. oleracea* L. leaf extract produces purer Ag NPs. This analysis agrees with the XRD analysis. Similar outcomes have been initiated by earlier studies [109].

3.3 | Enhancing light absorption properties of indium tin oxide (ITO) coated glass

After biosynthesizing Ag NPs from fresh and dry *P. oleracea* L. leaf extracts, it has been used through the spin-coating method and accumulated on the indium tin oxide (ITO) coated glass. The size of the ITO coated glass was 1 × 4.5 cm in order to be placed in the UV–vis cuvette place. The Ffirst 2 mg of Ag NPs, synthesized from fresh and dry *P. oleracea* L. leaf extracts independently, were mixed with 25 mL of ethanol and magnetically stirred at 40°C for 1 h till the mixture became an entirely monochrome solution. The ITO glass substrate was cleaned in acetone using an ultrasonic bath cleaner. Then the substrates were cleaned with double distilled water and then dehydrated

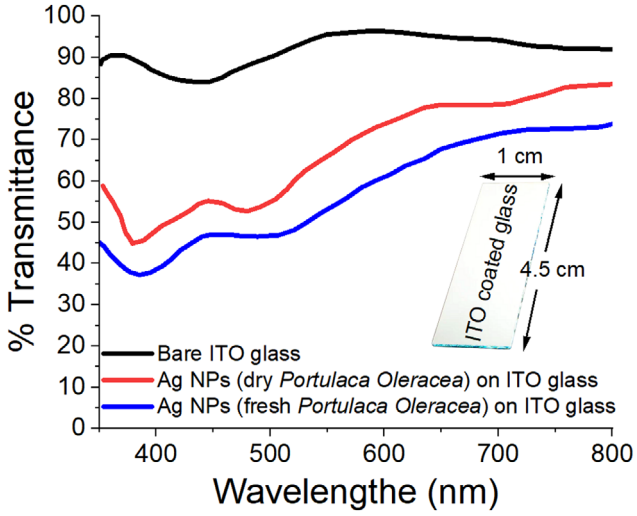

FIGURE 11 Transmittance spectra of bare and coated ITO glass using biosynthesized Ag NPs.

at ambient temperature. The dried substrate was stabilized on the spin coater disk. 1 mL of precursor solvent was added to the ITO glass substrate through injection at ≈3000 rpm for 1 min. Subsequently, the deposited film was dehydrated at 100°C for 2 min on the hot plate in order to remove any left behind components. Lastly, the prepared films were annealed at 300°C for 10 min in the oven to achieve a crystalline film. Then, the sample experienced gentle cooling at ambient temperature. This method is a time and cost-effective method to produce arbitrarily dispersed Ag NPs on the top of ITO glass, which can increase the absorption of ITO glass in the visible range of light.

Figure 11 shows the transmittance spectra of bare and coated ITO glass using biosynthesized Ag NPs from fresh and dry *P. oleracea* L. leaf extracts. It can be noticed, from Figure 11, that coating Ag NPs on the top of the ITO glass reduces the transmittance and hence enhancing the absorbance.

Consistent with the theory of localized surface plasmon resonance (LSPR), once Ag NPs are excited by incident light, they show cooperative oscillations of their conduction electrons that cause both absorption and scattering of the incident light

[114]. Accordingly, the transmittance of Ag NPs on ITO glass decreased from ≈90% to 55%, for dry *P. oleracea* L. leaf extract, and 45%, for fresh *P. oleracea* L. leaf extract, compared to bare ITO glass. This noticeable difference between Ag NPs synthesized from fresh and dry *P. oleracea* L. leaf extracts, is due to the fact that the LSPR phenomena is evidently rely upon the size and distribution of Ag NPs. Otherwise stated, the utilized Ag NPs, from fresh *P. oleracea* L. leaf extract, possesses smaller size as well as lower agglomeration, thus lower light transmittance. The anticipated process can be employed in constructing surface plasmonic resources with selective light absorption.

4 | CONCLUSION

In this investigation Ag NPs were effectively produced by means of green, environmentally friendly, easy, and cost-effective method. Fresh and dry *P. oleracea* L. leaf extracts have been utilized as reducing, capping and stabilizing agents. Diverse description methods were employed to explore the morphology, pureness, degree of crystallinity, structural, and optical characteristics of the green synthesized Ag NPs. This study showed that fresh *P. oleracea* L. leaf extract is a better medium to produce NPs that possess higher purity, stability, degree of crystallinity, and spherical shape. This is probably owing to the truth that throughout the drying procedure, the plant extract might lose some of the phytochemicals or convert them to another form, such as flavone to flavanone, that participating in reduction, capping, and stabilization processes. The biosynthesized Ag NPs from both mediums were coated on the ITO glass substrates to improve the reflection of ITO glass. It has been shown that the utilized Ag NPs, from fresh *P. oleracea* L. leaf extract, possesses smaller size as well as lower agglomeration, thus lower light transmittance. Finally, this process can scale up economic viability with high-quality products of different tunable bandgap.

AUTHOR CONTRIBUTIONS

Azeez A. Barzinjy: Supervision; conceptualization; writing—review editing and submission. **Banaz Sh. Haji**: Methodology; data curation; plotting graphs and experimental works.

ACKNOWLEDGEMENTS

The authors would like to thank Soran University, Tishk International University and Salahaddin University-Erbil for their unrestricted engorgements. A special thanks goes to Dr. David M.W. Waswa at Tishk International University for his excellent proofreading of this manuscript.

CONFLICT OF INTEREST STATEMENT

The authors report no conflicts of interest.

DATA AVAILABILITY STATEMENT

The data supporting the findings of the article is available within the article.

ORCID

Azeez A. Barzinjy https://orcid.org/0000-0003-4009-9845

REFERENCES

1. Bayda, S., et al.: The history of nanoscience and nanotechnology: From chemical-physical applications to nanomedicine. Molecules 25(1), 112 (2020)
2. Aithal, P.: Nanotechnology innovations and business opportunities: A review. Int. J. Manage., IT Eng. 6(1), 182–204 (2016)
3. Bocca, B., et al.: ICP-MS based methods to characterize nanoparticles of TiO2 and ZnO in sunscreens with focus on regulatory and safety issues. Sci. Total Environ. 630, 922–930 (2018)
4. Hussein, H.S.: The state of the art of nanomaterials and its applications in energy saving. Bull. Natl. Res. Cent. 47(1), 7 (2023)
5. Ahmad, A., et al.: Recent developments in metal/metalloid nanomaterials for battery applications; A comparative review. Fuel 340, 127399 (2023)
6. Kang, B.-H., et al.: Ultrafast and real-time nanoplasmonic on-chip polymerase chain reaction for rapid and quantitative molecular diagnostics. ACS Nano 15(6), 10194–10202 (2021)
7. Desai, N., et al.: Metallic nanoparticles as drug delivery system for the treatment of cancer. Expert Opin. Drug Delivery 18(9), 1261–1290 (2021)
8. Huang, Y.-C., et al.: Quantitative imaging of single light-absorbing nanoparticles by widefield interferometric photothermal microscopy. ACS Photonics 8(2), 592–602 (2021)
9. Samajdar, D.: Light-trapping strategy for PEDOT: PSS/c-Si nanopyramid based hybrid solar cells embedded with metallic nanoparticles. Sol. Energy 190, 278–285 (2019)
10. Sápi, A., et al.: Metallic nanoparticles in heterogeneous catalysis. Catal. Lett. 151(8), 2153–2175 (2021)
11. Haick, H.: Chemical sensors based on molecularly modified metallic nanoparticles. J. Phys. D: Appl. Phys. 40(23), 7173 (2007)
12. Khan, A.U., Khan, M., Khan, M.M.: Antifungal and antibacterial assay by silver nanoparticles synthesized from aqueous leaf extract of Trigonella foenum-graecum. J. Bionanosci. 9(3), 597–602 (2019)
13. Said, M.M., et al.: Multifunctional hydroxyapatite/silver nanoparticles/cotton gauze for antimicrobial and biomedical applications. Nanomaterials 11(2), 429 (2021)
14. Tehri, N., et al.: Biosynthesis, antimicrobial spectra and applications of silver nanoparticles: Current progress and future prospects. Inorg. Nano-Metal Chem. 52(1), 1–19 (2022)
15. Yuan, Y., et al.: Nano-silver functionalized polysaccharides as a platform for wound dressings: A review. Int. J. Biol. Macromol. 194, 644–653 (2022)
16. Jyoti, K., et al.: Antibacterial and anti-inflammatory activities of Cassia fistula fungal broth-capped silver nanoparticles. Mater. Technol. 36(14), 883–893 (2021)
17. Ali, S., et al.: Advancements and challenges in phytochemical-mediated silver nanoparticles for food packaging: Recent review (2021–2023). Trends Food Sci. Technol. 141, 104197 (2023)
18. Kaushal, A., et al.: Advances in therapeutic applications of silver nanoparticles. Chem. Biol. Interact. 382, 110590 (2023)
19. Mallineni, S.K., et al.: Silver nanoparticles in dental applications: A descriptive review. Bioengineering 10(3), 327 (2023)
20. Zhang, X.-F., et al.: Silver nanoparticles: Synthesis, characterization, properties, applications, and therapeutic approaches. Int. J. Mol. Sci. 17(9), 1534 (2016)
21. Nagajyothi, P.C., et al.: Green synthesis: Photocatalytic degradation of textile dyes using metal and metal oxide nanoparticles-latest trends and advancements. Crit. Rev. Environ. Sci. Technol. 50(24), 2617–2723 (2020)
22. Iravani, S., et al.: Synthesis of silver nanoparticles: Chemical, physical and biological methods. Res. Pharm. Sci. 9(6), 385 (2014)
23. Khan, M.M., et al.: Synthesis of cysteine capped silver nanoparticles by electrochemically active biofilm and their antibacterial activities. Bull. Korean Chem. Soc. 33(8), 2592–2596 (2012)

24. Pradeep, N., et al.: Investigation of microstructure and mechanical properties of microwave consolidated TiMgSr alloy prepared by high energy ball milling. Powder Technol. 408, 117715 (2022)
25. Palos, C.M.M., et al.: Large-scale production of ZnO nanoparticles by high energy ball milling. Physica B 656, 414776 (2023)
26. Parveen, K., Banse, V., Ledwani, L.: Green synthesis of nanoparticles: Their advantages and disadvantages. AIP Conf. Proc. 1724(1), 020048 (2016)
27. Chirumamilla, P., Dharavath, S.B., Taduri, S.: Eco-friendly green synthesis of silver nanoparticles from leaf extract of Solanum khasianum: Optical properties and biological applications. Appl. Biochem. Biotechnol. 195(1), 353–368 (2023)
28. Strapasson, G.B., et al.: Eco-friendly synthesis of silver nanoparticles and its application in hydrogen photogeneration and nanoplasmonic biosensing. ChemPhysChem 24(21), e202300002 (2023)
29. El-Shamy, O.A., Deyab, M.: Eco-friendly biosynthesis of silver nanoparticles and their improvement of anti-corrosion performance in epoxy coatings. J. Mol. Liq. 376, 121488 (2023)
30. Ahmad, R., et al.: Phytochemical delivery through nanocarriers: A review. Colloids Surf. B 197, 111389 (2021)
31. Chang, S.K., Alasalvar, C., Shahidi, F.: Review of dried fruits: Phytochemicals, antioxidant efficacies, and health benefits. J. Funct. Foods 21, 113–132 (2016)
32. Ta, C.A.K., Arnason, J.T.: Mini review of phytochemicals and plant taxa with activity as microbial biofilm and quorum sensing inhibitors. Molecules 21(1), 29 (2016)
33. Saratale, R.G., et al.: A comprehensive review on green nanomaterials using biological systems: Recent perception and their future applications. Colloids Surf. B 170, 20–35 (2018)
34. Javaid, A., et al.: Diversity of bacterial synthesis of silver nanoparticles. J. Bionanosci. 8(1), 43–59 (2018)
35. Truong, L.B., et al.: Cancer therapeutics with microbial nanotechnology-based approaches. In: Handbook of Microbial Nanotechnology, pp. 17–43. Elsevier, Amsterdam (2022)
36. Chugh, D., Viswamalya, V., Das, B.: Green synthesis of silver nanoparticles with algae and the importance of capping agents in the process. J. Genet. Eng. Biotechnol. 19(1), 1–21 (2021)
37. Khan, A.U., et al.: Fungi-assisted silver nanoparticle synthesis and their applications. Bioprocess. Biosyst. Eng. 41(1), 1–20 (2018)
38. Honary, S., et al.: Fungus-mediated synthesis of gold nanoparticles: A novel biological approach to nanoparticle synthesis. J. Nanosci. Nanotechnol. 13(2), 1427–1430 (2013)
39. Mourato, A., et al.: Biosynthesis of crystalline silver and gold nanoparticles by extremophilic yeasts. Bioinorg. Chem. Appl. 2011, 546074 (2011)
40. Saravanan, A., et al.: A review on biosynthesis of metal nanoparticles and its environmental applications. Chemosphere 264, 128580 (2020)
41. Varadharaj, V., et al.: Antidiabetic and antioxidant activity of green synthesized starch nanoparticles: An in vitro study. J. Cluster Sci. 31(6), 1257–1266 (2020)
42. Vijayaraghavan, K., Ashokkumar, T.: Plant-mediated biosynthesis of metallic nanoparticles: A review of literature, factors affecting synthesis, characterization techniques and applications. J. Environ. Chem. Eng. 5(5), 4866–4883 (2017)
43. El-Seedi, H.R., et al.: Metal nanoparticles fabricated by green chemistry using natural extracts: Biosynthesis, mechanisms, and applications. RSC Adv. 9(42), 24539–24559 (2019)
44. Honary, S., et al.: Development and optimization of biometal nanoparticles by using mathematical methodology: A microbial approach. J. Nano Res. 30, 106–115 (2015)
45. Virmani, I., et al.: Comparative anticancer potential of biologically and chemically synthesized gold nanoparticles. J. Cluster Sci. 31(4), 867–876 (2020)
46. Barabadi, H., et al.: Green nanotechnology-based gold nanomaterials for hepatic cancer therapeutics: A systematic review. Iran. J. Pharm. Res. 19(3), 3 (2020)
47. Barzinjy, A.A.: Characterization of ZnO nanoparticles prepared from green synthesis using Euphorbia Petiolata leaves. Eurasian J. Sci. Eng. 4(3), 74–83 (2019)
48. Ahmad, N., et al.: Rapid synthesis of silver nanoparticles using dried medicinal plant of basil. Colloids Surf. B 81(1), 81–86 (2010)
49. Noruzi, M.: Biosynthesis of gold nanoparticles using plant extracts. Bioprocess. Biosyst. Eng. 38(1), 1–14 (2015)
50. Tiwari, P., et al.: Phytochemical screening and extraction: A review. Int. Pharm. Sci. 1(1), 98–106 (2011)
51. Oikeh, E.I., Oviasogie, F.E., Omoregie, E.S.: Quantitative phytochemical analysis and antimicrobial activities of fresh and dry ethanol extracts of Citrus sinensis (L.) Osbeck (sweet Orange) peels. Clin. Phytosci. 6(1), 1–6 (2020)
52. Fahimirad, S., Ajalloueian, F., Ghorbanpour, M.: Synthesis and therapeutic potential of silver nanomaterials derived from plant extracts. Ecotoxicol. Environ. Saf. 168, 260–278 (2019)
53. Tang, X., et al.: Enhancing absorption properties of composite nanosphere and nanowire arrays by localized surface plasmon resonance shift. Result Phys. 7, 87–94 (2017)
54. Barzinjy, A.A.: Structure, synthesis and applications of ZnO nanoparticles: A review. Jordan J. Phys. 13(2), 123–135 (2020)
55. Azeez, H.H., Barzinjya, A.A.: Biosynthesis zinc oxide nanoparticles using Apium graveolens L. leaf extract and its use in removing the organic pollutants in water. Desalin. Water Treat. 190, 179–192 (2020)
56. Barzinjy, A.A., et al.: Green synthesis of the magnetite (Fe3O4) nanoparticle using Rhus coriaria extract: A reusable catalyst for efficient synthesis of some new 2-naphthol bis-Betti bases. Inorg. Nano-Metal Chem. 50(8), 620–629 (2020)
57. Barzinjy, A.A., Azeez, H.H.: Green synthesis and characterization of zinc oxide nanoparticles using Eucalyptus globulus Labill. leaf extract and zinc nitrate hexahydrate salt. SN Appl. Sci. 2(5), 1–14 (2020)
58. Barzinjy, A.A., et al.: Biosynthesis, characterization and mechanism of formation of ZnO nanoparticles using Petroselinum crispum leaf extract. Curr. Org. Synth. 17(7), 558–566 (2020)
59. Barzinjy, A.A., et al.: Green and eco-friendly synthesis of Nickel oxide nanoparticles and its photocatalytic activity for methyl orange degradation. J. Mater. Sci.: Mater. Electron. 31, 11303–11316 (2020)
60. Barzinjy, A.A., et al.: Biosynthesis and characterisation of zinc oxide nanoparticles from Punica granatum (pomegranate) juice extract and its application in thin films preparation by spin-coating method. Nano Lett. 15(6), 415–420 (2020)
61. Nasrollahzadeh, M., et al.: Biosynthesis of the palladium/sodium borosilicate nanocomposite using Euphorbia milii extract and evaluation of its catalytic activity in the reduction of chromium (VI), nitro compounds and organic dyes. Mater. Res. Bull. 102, 24–35 (2018)
62. Talabani, R.F., et al.: Biosynthesis of silver nanoparticles and their applications in harvesting sunlight for solar thermal generation. Nanomaterials 11(9), 2421 (2021)
63. Shnawa, B.H., et al.: Scolicidal activity of biosynthesized zinc oxide nanoparticles by Mentha longifolia L. leaves against Echinococcus granulosus protoscolices. Emergent Mater. 5, 683–693 (2021)
64. Ahangarpour, A., et al.: Effects of Portulaca oleracea ethanolic extract on reproductive system of aging female mice. Int. J. Reprod. Biomed. 14(3), 205 (2016)
65. Gulrajani, M., et al.: Preparation and application of silver nanoparticles on silk for imparting antimicrobial properties. J. Appl. Polym. Sci. 108(1), 614–623 (2008)
66. Velusamy, B., Kaliyaperumal, S., Raju, A.: Collection and data-mining of bioactive compounds with cancer treatment properties in the plants of Fabaceae family. Int. J. Pharm. Sci. Res. 7(5), 2065 (2016)
67. Dhivya, S., Kalaichelvi, K.: UV-Vis spectroscopic and FTIR analysis of Sarcostemma brevistigma, wight. and arn. Int. J. Herb. Med. 9(3), 46–49 (2017)
68. Rani, N., Sharma, S., Sharma, M.: Phytochemical analysis of Meizotropis pellita by FTIR and UV-Vis spectrophotometer. Indian J. Sci. Technol. 9(31), 1–4 (2016)

69. Zhu, H., et al.: Analysis of flavonoids in Portulaca oleracea L. by UV-vis spectrophotometry with comparative study on different extraction technologies. Food Anal. Methods 3(2), 90–97 (2010)
70. Nibbs, A.E., Scheidt, K.A.: Asymmetric methods for the synthesis of flavanones, chromanones, and azaflavanones. Eur. J. Org. Chem. 2012. (3), 449–462 (2012)
71. Romani, A., et al.: HPLC analysis of flavonoids and secoiridoids in leaves of Ligustrum vulgare L.(Oleaceae). J. Agric. Food Chem. 48(9), 4091–4096 (2000)
72. Donkor, S., et al.: Phytochemical, antimicrobial, and antioxidant profiles of Duranta erecta L. parts. Biochem. Res. Int. 2019, 8731595 (2019)
73. Restrepo, C.V., Villa, C.C.: Synthesis of silver nanoparticles, influence of capping agents, and dependence on size and shape: A review. Environ. Nanotechnol. Monit. Manage. 15, 100428 (2021)
74. Oliveira-Alves, S.C., et al.: Impact of drying processes on the nutritional composition, volatile profile, phytochemical content and bioactivity of Salicornia ramosissima j. Woods. Antioxidants 10(8), 1312 (2021)
75. Barabadi, H., et al.: Antineoplastic biogenic silver nanomaterials to combat cervical cancer: A novel approach in cancer therapeutics. J. Cluster Sci. 31(4), 659–672 (2020)
76. Ider, M., et al.: Silver metallic nanoparticles with surface plasmon resonance: Synthesis and characterizations. J. Cluster Sci. 28(3), 1051–1069 (2017)
77. Mourdikoudis, S., Pallares, R.M., Thanh, N.T.: Characterization techniques for nanoparticles: Comparison and complementarity upon studying nanoparticle properties. Nanoscale 10(27), 12871–12934 (2018)
78. Kamarudin, D., et al.: Synthesis of silver nanoparticles stabilised by PVP for polymeric membrane application: A comparative study. Mater. Technol. 37(5), 1–13 (2021)
79. Li, G., et al.: Fungus-mediated green synthesis of silver nanoparticles using Aspergillus terreus. Int. J. Mol. Sci. 13(1), 466–476 (2012)
80. Carson, L., et al.: Green synthesis of silver nanoparticles with antimicrobial properties using Phyla dulcis plant extract. Foodborne Pathog. Dis. 17(8), 504–511 (2020)
81. Remya, V., et al.: Silver nanoparticles green synthesis: A mini review. Chem. Int. 3(2), 165–171 (2017)
82. Danaei, M., et al.: Impact of particle size and polydispersity index on the clinical applications of lipidic nanocarrier systems. Pharmaceutics 10(2), 57 (2018)
83. Mohanpuria, P., Rana, N.K., Yadav, S.K.: Biosynthesis of nanoparticles: Technological concepts and future applications. J. Nanopart. Res. 10(3), 507–517 (2008)
84. Hanarp, P., et al.: Influence of polydispersity on adsorption of nanoparticles. J. Colloid Interface Sci. 241(1), 26–31 (2001)
85. Banerjee, S., Maity, A., Chakravorty, D.: Quantum confinement effect in heat treated silver oxide nanoparticles. J. Appl. Phys. 87(12), 8541–8544 (2000)
86. Banerjee, R., Jayakrishnan, R., Ayyub, P.: Effect of the size-induced structural transformation on the band gap in CdS nanoparticles. J. Phys. Condens. Matter 12(50), 10647 (2000)
87. Pryshchepa, O., Pomastowski, P., Buszewski, B.: Silver nanoparticles: Synthesis, investigation techniques, and properties. Adv. Colloid Interface Sci. 284, 102246 (2020)
88. Giannini, V., et al.: Plasmonic nanoantennas: Fundamentals and their use in controlling the radiative properties of nanoemitters. Chem. Rev. 111(6), 3888–3912 (2011)
89. Sarina, S., Waclawik, E.R., Zhu, H.: Photocatalysis on supported gold and silver nanoparticles under ultraviolet and visible light irradiation. Green Chem. 15(7), 1814–1833 (2013)
90. Gharibshahi, L., et al.: Structural and optical properties of Ag nanoparticles synthesized by thermal treatment method. Materials 10(4), 402 (2017)
91. Gharibshahi, E., Saion, E.: Influence of dose on particle size and optical properties of colloidal platinum nanoparticles. Int. J. Mol. Sci. 13(11), 14723–14741 (2012)
92. Evanoff, D.D. Jr, Chumanov, G.: Synthesis and optical properties of silver nanoparticles and arrays. ChemPhysChem 6(7), 1221–1231 (2005)
93. Aziz, A., et al.: Structural, morphological and optical investigations of silver nanoparticles synthesized by sol-gel auto-combustion method. Dig. J. Nanomater. Biostruct. 13(3), 679–683 (2018)
94. Mistry, H., et al.: Biogenically proficient synthesis and characterization of silver nanoparticles employing marine procured fungi Aspergillus brunneoviolaceus along with their antibacterial and antioxidative potency. Biotechnol. Lett. 43(1), 307–316 (2021)
95. Senthil, B., et al.: Non-cytotoxic effect of green synthesized silver nanoparticles and its antibacterial activity. J. Photochem. Photobiol. B 177, 1–7 (2017)
96. He, Y., et al.: Green synthesis of silver nanoparticles by Chrysanthemum morifolium Ramat. extract and their application in clinical ultrasound gel. Int. J. Nanomed. 8, 1809 (2013)
97. Wahab, A.W., Karim, A., Sutapa, I.W.: Bio-synthesis of gold nanoparticles through bioreduction using the aqueous extract of Muntingia calabura L. leaf. Orient. J. Chem. 34(1), 401 (2018)
98. Mallikarjuna, K., et al.: Green synthesis of silver nanoparticles using Ocimum leaf extract and their characterization. Dig. J. Nanomater. Biostruct. 6(1), 181–186 (2011)
99. Jemal, K., Sandeep, B., Pola, S.: Synthesis, characterization, and evaluation of the antibacterial activity of Allophylus serratus leaf and leaf derived callus extracts mediated silver nanoparticles. J. Nanomater. 2017, 4213275 (2017)
100. Jyoti, K., Baunthiyal, M., Singh, A.: Characterization of silver nanoparticles synthesized using Urtica dioica Linn. leaves and their synergistic effects with antibiotics. J. Radiat. Res. Appl. Sci. 9(3), 217–227 (2016)
101. Eltarahony, M., et al.: Antibacterial, antifungal and antibiofilm activities of silver nanoparticles supported by crude bioactive metabolites of bionanofactories isolated from lake Mariout. Molecules 26(10), 3027 (2021)
102. Alsharif, S.M., et al.: Multifunctional properties of spherical silver nanoparticles fabricated by different microbial taxa. Heliyon 6(5), e03943 (2020)
103. Salem, S.S., et al.: Bactericidal and in-vitro cytotoxic efficacy of silver nanoparticles (Ag-NPs) fabricated by endophytic actinomycetes and their use as coating for the textile fabrics. Nanomaterials 10(10), 2082 (2020)
104. Aref, M.S., Salem, S.S.: Bio-callus synthesis of silver nanoparticles, characterization, and antibacterial activities via Cinnamomum camphora callus culture. Biocatal. Agric. Biotechnol. 27, 101689 (2020)
105. Bakhtiari-Sardari, A., et al.: Comparative evaluation of silver nanoparticles biosynthesis by two cold-tolerant Streptomyces strains and their biological activities. Biotechnol. Lett. 42, 1985–1999 (2020)
106. Satyavani, K., Ramanathan, T., Gurudeeban, S.: Green synthesis of silver nanoparticles by using stem derived callus extract of bitter apple (Citrullus colocynthis). Dig. J. Nanomater. Biostruct. 6(3), 1019–1024 (2011)
107. Gavade, S.M., et al.: Green synthesis of silver nanoparticles by using carambola fruit extract and their antibacterial activity. Adv. Nat. Sci.: Nanosci. Nanotechnol. 6(4), 045015 (2015)
108. Raza, M.A., et al.: Size-and shape-dependent antibacterial studies of silver nanoparticles synthesized by wet chemical routes. Nanomaterials 6(4), 74 (2016)
109. Ahani, M., Khatibzadeh, M.: Optimisation of significant parameters through response surface methodology in the synthesis of silver nanoparticles by chemical reduction method. Nano Lett. 12(9), 705–710 (2017)
110. El-Naggar, N.E.A., et al.: Production, extraction and characterization of Chlorella vulgaris soluble polysaccharides and their applications in AgNPs biosynthesis and biostimulation of plant growth. Sci. Rep. 10(1), 1–19 (2020)
111. Ajitha, B., et al.: Role of capping agents in controlling silver nanoparticles size, antibacterial activity and potential application as optical hydrogen peroxide sensor. RSC Adv. 6(42), 36171–36179 (2016)
112. Khan, I., Saeed, K., Khan, I.: Nanoparticles: Properties, applications and toxicities. Arabian J. Chem. 12(7), 908–931 (2019)

113. Jeevanandam, J., et al.: Review on nanoparticles and nanostructured materials: History, sources, toxicity and regulations. Beilstein J. Nanotechnol. 9(1), 1050–1074 (2018)
114. Song, E., et al.: Enhancement of photoconversion efficiency of CdSe quantum dots sensitized Al doped ZnO/Si heterojunction device decorated with Ag nanostructures. Mater. Sci. Semicond. Process. 149, 106878 (2022)

How to cite this article: Barzinjy, A.A., Haji, B.S.: Green synthesis and characterization of ag nanoparticles using fresh and dry *Portulaca Oleracea* leaf extracts: Enhancing light reflectivity properties of ITO glass. Micro Nano Lett. 19, e12198 (2024). https://doi.org/10.1049/mna2.12198